

# Deficiency of plasminogen activator inhibitor-2 results in accelerated tumor growth

Randal J. Westrick<sup>1,2,3</sup>   | Lisa Payne Røjkjær<sup>4</sup> | Angela Y. Yang<sup>4</sup> | Michael H. Roh<sup>5</sup> | Amy E. Siebert<sup>1</sup>  | David Ginsburg<sup>4,6,7</sup>

<sup>1</sup>Department of Biological Sciences, Oakland University, Rochester, Michigan

<sup>2</sup>Department of Bioengineering, Oakland University, Rochester, Michigan

<sup>3</sup>Centers for Data Science and Big Data Analytics and Biomedical Research, Oakland University, Rochester, Michigan

<sup>4</sup>Life Sciences Institute, University of Michigan, Ann Arbor, Michigan

<sup>5</sup>Department of Pathology, University of Michigan, Ann Arbor, Michigan

<sup>6</sup>Howard Hughes Medical Institute, University of Michigan, Ann Arbor, Michigan

<sup>7</sup>Departments of Human Genetics, Internal Medicine and Pediatrics, University of Michigan, Ann Arbor, Michigan

## Correspondence

David Ginsburg, Departments of Internal Medicine and Human Genetics, Howard Hughes Medical Institute, Life Sciences Institute, University of Michigan, 5214 LSI Building, 210 Washtenaw Avenue, Ann Arbor, MI 48109 USA.  
Email: ginsburg@umich.edu

Randal J. Westrick, Departments of Biological Sciences and Bioengineering, Oakland University, 305 Dodge Hall, 118 Library Drive, Rochester, MI 48309-4479, USA.  
Email: rjwestrick@oakland.edu

## Funding information

National Heart, Lung, and Blood Institute, Grant/Award Number: R01-HL135035 and R35-HL135793; American Heart Association, Grant/Award Number: 17IRG33460238; National Cancer Institute, Grant/Award Number: P30CA046592

## Abstract

**Background:** Upregulation of the plasminogen activation system, including urokinase plasminogen activator (uPA), has been observed in many malignancies, suggesting that co-opting the PA system is a common method by which tumor cells accomplish extracellular matrix proteolysis. PAI-2, a serine protease inhibitor, produced from the *SERPINB2* gene, inhibits circulating and extracellular matrix-tethered uPA. Decreased *SERPINB2* expression has been associated with increased tumor invasiveness and metastasis for several types of cancer. PAI-2 deficiency has not been reported in humans and PAI-2-deficient (*SerpB2*<sup>-/-</sup>) mice exhibit no apparent abnormalities.

**Objectives:** We investigated the role of PAI-2 deficiency on tumor growth and metastasis.

**Methods:** To explore the long-term impact of PAI-2 deficiency, a cohort of *SerpB2*<sup>-/-</sup> mice were aged to >18 months, with spontaneous malignancies observed in 4/9 animals, all of apparently vascular origin. To further investigate the role of PAI-2 deficiency in malignancy, *SerpB2*<sup>-/-</sup> and wild-type control mice were injected with either B16 melanoma or Lewis lung carcinoma tumor cells, with markedly accelerated tumor growth observed in *SerpB2*<sup>-/-</sup> mice for both cell lines. To determine the relative contributions of PAI-2 from hematopoietic or nonhematopoietically derived sources, bone marrow transplants between wild-type C57BL/6J and *SerpB2*<sup>-/-</sup> mice were performed.

**Results and Conclusions:** Our results suggest that PAI-2 deficiency increases susceptibility to spontaneous tumorigenesis in the mouse, and demonstrate that *SerpB2* expression derived from a nonhematopoietic compartment is a key host factor in the regulation of tumor growth in both the B16 melanoma and Lewis lung carcinoma models.

## KEYWORDS

cancer, fibrinolysis, PAI-2, serine protease inhibitor, tumor

R.J.W. and L.P.R. contributed equally to this work.

Manuscript handled by: Ton Lisman

Final decision: Ton Lisman, 03 August 2020

© 2020 International Society on Thrombosis and Haemostasis

## 1 | INTRODUCTION

Components of the plasminogen activation (PA) system, including urokinase plasminogen activator (uPA), are thought to play key roles in malignant tumor growth and metastasis.<sup>1</sup> Plasminogen activator inhibitor 2 (PAI-2), a serine protease inhibitor (SERPIN) produced by the *SERPINB2* gene, is a potent inhibitor of uPA.<sup>1</sup> PAI-2 is a predominantly intracellular SERPIN whose expression is induced by inflammatory mediators.<sup>2</sup> It is one of the most highly upregulated transcripts in activated macrophages and keratinocytes and is also highly inducible in fibroblasts and endothelial cells.<sup>2</sup> PAI-2 exists in two forms: a 47-kD nonglycosylated intracellular form, and a secreted 60-kD glycosylated form, though neither is generally detectable in plasma, except during pregnancy.<sup>3</sup> The regulation of *SERPINB2* gene expression is complex, with known induction by a variety of inflammatory molecules including tumor necrosis factor alpha (TNF- $\alpha$ ) and lipopolysaccharide.<sup>2</sup> Though PAI-2 is an efficient inhibitor of uPA, additional target proteases may exist in vivo, including several putative intracellular proteases.<sup>2,4</sup>

Clinical studies in breast, lung, and ovarian cancer patients have shown a striking correlation of low tumor-associated PAI-2 levels with poor prognosis, including increased lymph node involvement and decreased overall survival.<sup>2,5,6</sup> Expression of *SERPINB2* in several cell types in the context of the local tumor environment could potentially prevent malignant cell invasion.<sup>7</sup> Extracellular matrix degradation by colon carcinoma and monocyte invasion into human amniotic membranes is inhibited in the presence of exogenous PAI-2.<sup>8</sup> Transfection of *SERPINB2* into melanoma and sarcoma cell lines resulted in decreased ability to degrade extracellular matrix and a reduced capacity for metastasis.<sup>2</sup> Similarly, gene transfer of *Serp1nB2* into the liver was demonstrated to reduce fibrosarcoma primary tumor size in nude mice and significantly decrease the incidence of metastasis.<sup>2</sup> In addition, the plasminogen activation system has been demonstrated to play a prominent role in tumor progression in the mouse transplantable B16 melanoma and Lewis lung carcinoma tumor models.<sup>2,9,10</sup> Taken together, these observations suggest that localization of PAI-2 within the tumor microenvironment may play an important role in the regulation of tumor growth.

Though PAI-2 deficiency has not been reported in humans, PAI-2-deficient (*Serp1nB2*<sup>-/-</sup>) mice exhibit normal development and survival, as well as normal wound healing and response to infectious challenge.<sup>11</sup> In the present study, spontaneous tumors were observed in a subset of aging *Serp1nB2*<sup>-/-</sup> mice (>1 year of age). Analysis of wild-type (WT) control and *Serp1nB2*<sup>-/-</sup> mice challenged by injection with either B16 melanoma or Lewis lung carcinoma (LLC) cells, as well as chimeric animals generated by bone marrow transplant (BMT), suggest that *Serp1nB2* expression within a nonhematopoietically derived host compartment plays a key role in the limitation of tumor growth and metastasis in the mouse.

### Essentials

- Low PAI-2 (*SERPINB2*) is associated with increased tumor growth and metastasis.
- Aged PAI-2 deficient (*Serp1nB2*<sup>-/-</sup>) mice spontaneously develop tumors.
- *Serp1nB2*<sup>-/-</sup> mice display accelerated B16 melanoma or Lewis lung carcinoma growth.
- Non-hematopoietic PAI-2 regulates B16 melanoma and Lewis Lung carcinoma tumor growth.

## 2 | RESULTS

### 2.1 | Spontaneous tumor development in *Serp1nB2*<sup>-/-</sup> mice

A cohort of 9 male *Serp1nB2*<sup>-/-</sup> mice were observed until the cutoff date of 22 months of age with 44% (4 of 9) developing a spontaneous malignant tumor between 18 and 22 months. Three of these four tumors exhibited the histological appearance of angiosarcomas (Figure 1), with one tumor originating in the liver, another in the periarticular region of the hip, and one in both the liver and the flank. The fourth animal developed a large polyploid tumor in the dorsal flank that was classified as a fibrosarcoma. In contrast, as reported by Rudolph et al, the expected rate of spontaneous tumors in a mixed B6129 background (similar to the aged *Serp1nB2*<sup>-/-</sup> mice), is ~ 3% (2 of 63) mice. In addition, the *Serp1nB2*<sup>-/-</sup> mice had a higher rate of spontaneous tumor formation than homozygous telomerase-deficient mice (mTR<sup>-/-</sup>) and unlike the more common tumor types observed in aging B6129 mice, exhibited rare angio- and fibrosarcomas.<sup>12,13</sup>

### 2.2 | Enhanced growth of heterologous tumors in *Serp1nB2*<sup>-/-</sup> mice

To investigate the role of PAI-2 in the host response to exogenously introduced tumor cells, male *Serp1nB2*<sup>-/-</sup> mice and littermate controls from an intercross of *Serp1nB2*<sup>+/+</sup> mice backcrossed three generations to C57BL/6J (N3) were challenged by left hind footpad inoculation of B16 melanoma cells<sup>14</sup> (derived from C57BL/6J mice). All 7 *Serp1nB2*<sup>-/-</sup> mice and three of five WT littermate controls developed visible tumors by 34 days postinoculation, with significantly larger tumor size observed in the *Serp1nB2*<sup>-/-</sup> mice (Figure 2A; mean tumor volume in *Serp1nB2*<sup>-/-</sup> recipients = 292  $\pm$  58 mm<sup>3</sup> vs WT control mice = 16  $\pm$  9 mm<sup>3</sup>;  $P < .003$ ). In addition, two of seven *Serp1nB2*<sup>-/-</sup> mice developed numerous lung metastases with chest wall involvement, with no lung metastases observed among the five WT controls. The local footpad tumors in the *Serp1nB2*<sup>-/-</sup> mice appeared highly invasive, with infiltration between smooth muscle bundles and extension into the subepidermal layer, in contrast to a circumscribed appearance in

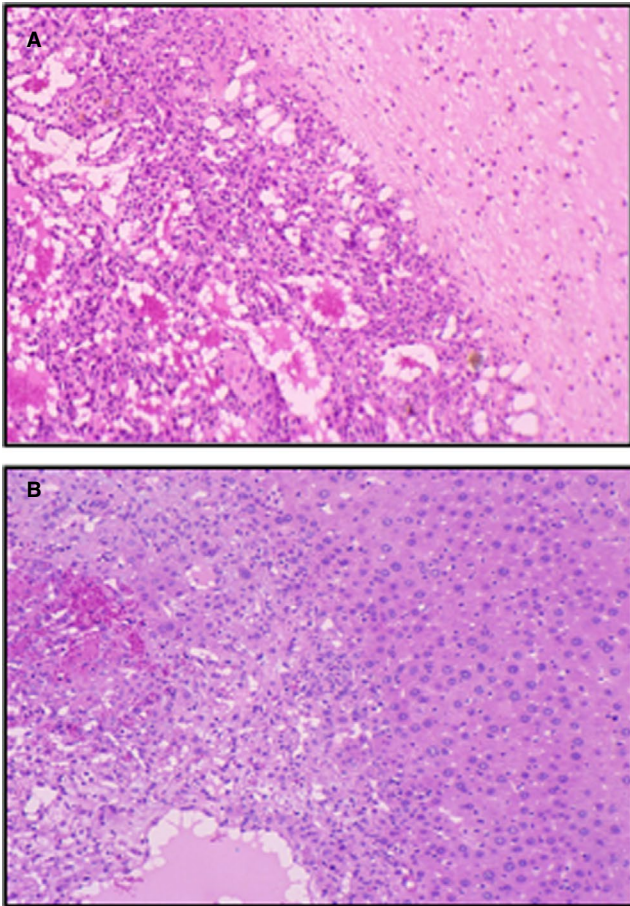


**FIGURE 1** Histological examination of spontaneous tumors arising in aged *SerpinB2*<sup>-/-</sup> mice. Hematoxylin and eosin staining of zinc formalin-fixed, paraffin-embedded tumors pathologically defined as angiosarcomas, which developed in the (A) hip and (B) liver in two independent animals

the WT mice (Figure 3A-D). In two *SerpinB2*<sup>-/-</sup> mice, the inoculated footpad melanoma extended into the leg and hip, a finding not seen in any of the five control mice.

To address the potential confounding effects of the mixed 129/C57BL/6J strain background, a second set of experiments were conducted in mice after 7 backcross generations into C57BL/6J (N7), including 9 *SerpinB2*<sup>-/-</sup> mice, 8 heterozygous *SerpinB2*<sup>±</sup> littermates, and 13 WT littermate controls. Visible tumors developed in 8/13 WT, 9/9 *SerpinB2*<sup>-/-</sup>, and 8/8 heterozygous mice (Figure 2B). Numerous lung metastases developed in three of nine *SerpinB2*<sup>-/-</sup> mice, but in none of the heterozygotes or WT controls. A significant increase in mean local tumor volume was again observed in *SerpinB2*<sup>-/-</sup> mice compared to WT controls with intermediate values in the heterozygotes (Figure 2B; mean tumor volume: *SerpinB2*<sup>-/-</sup> 214 ± 42 mm<sup>3</sup>, *SerpinB2*<sup>±</sup> 83 ± 20 mm<sup>3</sup>, WT 31 ± 13 mm<sup>3</sup>). One *SerpinB2*<sup>-/-</sup> mouse was euthanized at day 28 because of extensive tumor invasion from the footpad into the leg, and was excluded from evaluation.

Similar sets of experiments were performed in *SerpinB2*<sup>-/-</sup> and WT mice using LLC injected either into the footpad or intradermally

on the back (Figure 2C,D). A highly significant increase in local tumor growth was observed in N3 *SerpinB2*<sup>-/-</sup> mice compared with WT littermate controls at both sites of tumor administration, associated with a more invasive histological appearance (Figure 3E,F). Two of four *SerpinB2*<sup>-/-</sup> mice inoculated intradermally exhibited progression of LLC tumor to the spine, a finding not seen in any of the WT controls.

### 2.3 | The optimal host response to injected B16 melanoma or LLC tumor cells requires *SerpinB2* expression by nonhematopoietically derived host cells

*SerpinB2* is highly expressed in macrophages,<sup>15-17</sup> suggesting a potential role for these or other hematopoietically derived cells in the host responses to B16 melanoma and LLC observed above. To test this hypothesis, BMT was performed into N7 *SerpinB2*<sup>-/-</sup> recipients and age and sex-matched WT littermate controls using either donor *SerpinB2*<sup>-/-</sup> or WT fetal liver cells (FLC). All four sham-transplanted mice died within 4 days of irradiation, demonstrating effective myeloablation. There was no mortality among the other transplanted groups. WT mice receiving *SerpinB2*<sup>-/-</sup> FLC should be *SerpinB2*-deficient in all cell populations of hematopoietic origin with normal expression in all other cell types, whereas *SerpinB2*<sup>-/-</sup> mice reconstituted with WT FLC should exhibit the converse pattern, with normal *SerpinB2* expression restricted to cells of hematopoietic origin including monocytes/macrophages (Figure 4). Footpad injections of B16 melanoma cells were performed 6 weeks after BMT *SerpinB2*<sup>-/-</sup> mice reconstituted with WT FLCs demonstrate accelerated tumor growth similar to that observed in untransplanted *SerpinB2*<sup>-/-</sup> mice or *SerpinB2*<sup>-/-</sup> mice reconstituted with *SerpinB2*<sup>-/-</sup> FLCs (Figure 4; compared with Figure 2B). In contrast, WT mice receiving either *SerpinB2*<sup>-/-</sup> or WT FLCs exhibited reduced tumor volume (Figure 4), similar to untransplanted WT mice (Figure 2).

## 3 | DISCUSSION

Although decreased *SerpinB2* expression has been repeatedly associated with poor cancer prognosis,<sup>2</sup> the role of PAI-2 in human tumors is unclear. In a comprehensive analysis of multiple cancer types, mutations in SERPINB2 were not identified as “tumor drivers.”<sup>18</sup> Similarly, heterozygosity for germline *SerpinB2* loss-of-function mutations is observed in the general population with a frequency of ~1:2500,<sup>19</sup> and would be expected to result in a familial cancer predisposition syndrome with a similar frequency, if PAI-2 functioned as a tumor suppressor.

These data suggest a regulatory function for *SerpinB2* expression in nontumor cell types, potentially playing a role in host defense. Consistent with this hypothesis, analysis of PAI-2 in tumor sections is associated with stromal cells such as endothelial cell, fibroblasts, and macrophages.<sup>2</sup> The observation that heterozygous *SerpinB2*<sup>±</sup> mice demonstrate an invasive B16 melanoma phenotype

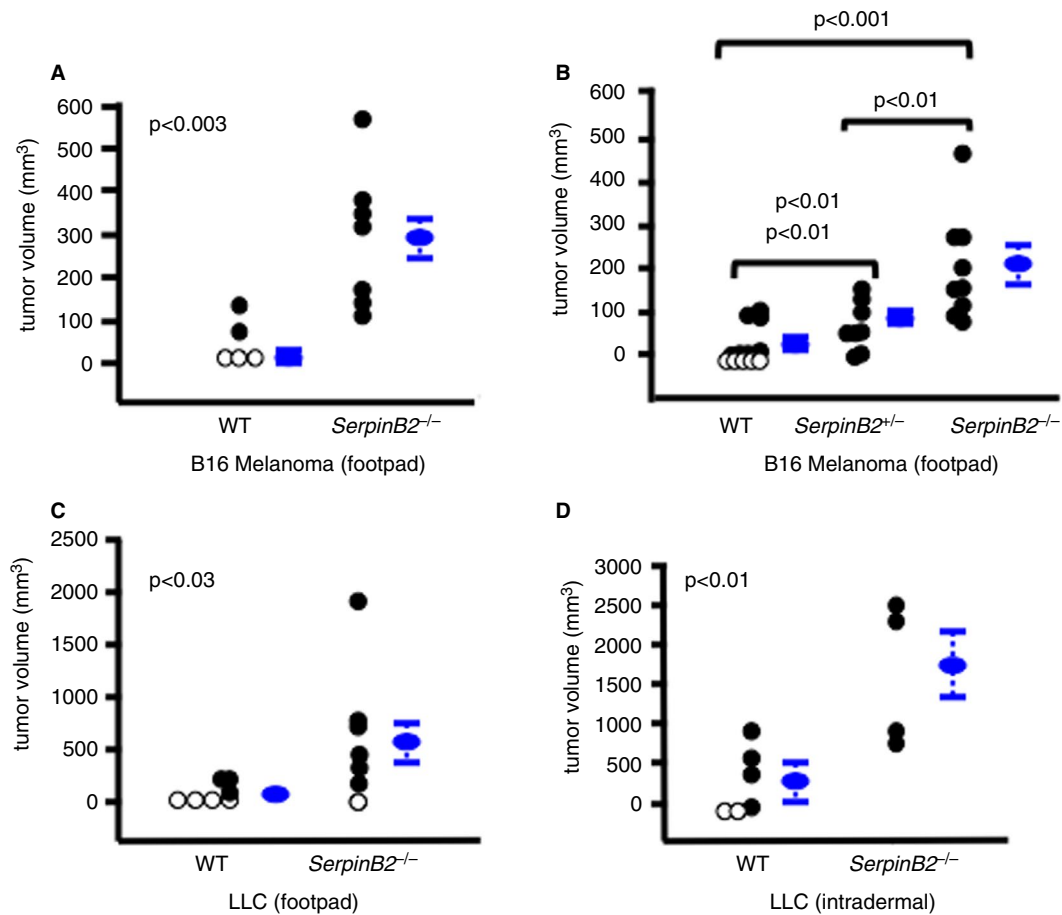


**FIGURE 2** Host *SerpinB2* status modulates primary tumor size. B16 melanoma or Lewis lung carcinoma was injected into (A-C) the left hind footpad or (D) the dorsal intradermal region of each animal. Mice with tumors are represented by solid symbols; mice that did not develop tumors are indicated with open symbols. Panels A and B are the results of B16 melanoma experiments; panels C and D are the results of the LLC experiments. A. N3 *SerpinB2*<sup>-/-</sup> mice had a mean tumor volume = 292 mm<sup>3</sup> vs 16 mm<sup>3</sup> in WT mice;  $P < .003$ . B. N7 *SerpinB2*<sup>-/-</sup> mean tumor volume 214 mm<sup>3</sup> vs *SerpinB2*<sup>+/-</sup> 83 mm<sup>3</sup>;  $P < .01$ , *SerpinB2*<sup>+/-</sup> vs WT 31 mm<sup>3</sup>;  $P < .01$ , *SerpinB2*<sup>-/-</sup> vs WT  $P < .001$ . Tumor volumes were calculated at day 34. One *SerpinB2*<sup>-/-</sup> mouse was euthanized at day 28 because of extensive tumor spread throughout the leg, and was excluded from evaluation. C. Mean footpad LLC volume (day 31) N3 *SerpinB2*<sup>-/-</sup> 718 mm<sup>3</sup> vs WT 72 mm<sup>3</sup>;  $P < .03$ . D. Mean dorsal intradermal LLC volume (day 22) N3 *SerpinB2*<sup>-/-</sup> 1735 mm<sup>3</sup> vs WT 348 mm<sup>3</sup>;  $P < .01$ . Error bars indicate standard error of the mean

intermediate between those of *SerpinB2*<sup>-/-</sup> and WT mice suggests a gene dosage effect.

Given the known expression of *SERPINB2* in a number of hematopoietically derived cell types, including monocyte/macrophages and stem cells,<sup>2</sup> the observation that BMT of WT FLCs into *SerpinB2*<sup>-/-</sup> (or *SerpinB2*<sup>-/-</sup> FLCs into WT) mice had no effect on B16 melanoma or LLC tumor growth was surprising. These data demonstrate that the accelerated tumor growth observed in *SerpinB2*<sup>-/-</sup> mice is not due to a specific deficiency within the macrophage or another hematopoietically derived cell population, but rather from a nonhematopoietically derived source. However, we cannot exclude a role for memory T-lymphocytes or tissue phase macrophages, which, although hematopoietically derived, turn over at very low rates and propagate by self-renewal in tissues.<sup>20</sup> The spontaneous development of tumors in aged *SerpinB2*<sup>-/-</sup> mice is also consistent with an important role for *SerpinB2* gene expression by a nonhematopoietic host cell compartment in naturally

occurring cancers, in addition to exogenously introduced cancer models. These data raise the possibility of an important role for PAI-2 produced by stromal cells within the tumor microenvironment.<sup>2</sup> Recently, Harris et al demonstrated that stromal cell PAI-2 is required for normal collagen remodeling in vitro, establishing a novel role for stromal PAI-2 in tumor growth and invasion.<sup>21</sup>

Mechanistically, it is possible that PAI-2 could affect tumor growth via a function unrelated to plasminogen activator inhibition. These functional roles could partially or wholly contribute to the inhibition of tumorigenesis and growth. The intracellular localization of PAI-2 suggests that it could function to regulate intracellular processes impacting tumor growth.<sup>22</sup> For example, PAI-2 has previously been shown to inhibit TNF- $\alpha$ -induced apoptosis,<sup>23,24</sup> as well as acting as a downstream effector of p38 signaling to maintain macrophage survival during *Bacillus anthracis* triggered apoptosis.<sup>25</sup> Similarly, PAI-2 has also been shown to maintain the survival of TNF-stimulated cells by stabilizing transglutaminase 2 through interaction with PAI-2's C-D interhelical



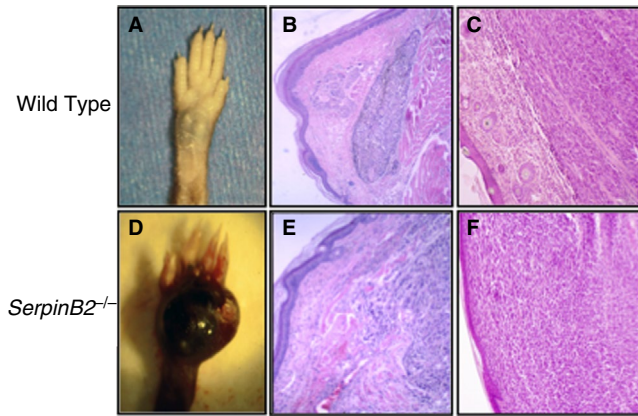


**FIGURE 3** Gross and histological examination of footpad tumors following injection with B16 melanoma or LLC. Representative (A) WT or (B) *SerpinB2*<sup>-/-</sup> mice at day 34. Hematoxylin and eosin staining of zinc formalin-fixed, paraffin-embedded tissue from a day 34 footpad tumor of a (C) WT and (D) *SerpinB2*<sup>-/-</sup> mouse showing a well-circumscribed area of tumor in panel C compared with a much more invasive appearance of the melanoma in the *SerpinB2*<sup>-/-</sup> mouse (D). Similarly, compared with (E) WT, (F) LLC exhibited more invasive growth in a *SerpinB2*<sup>-/-</sup> mouse at day 31

domain, leading to caspase 3 inactivation by transglutaminase 2 and increased survival.<sup>26</sup> Loss of PAI-2 may also lead to loss of retinoblastoma-mediated repression of proapoptotic gene transcription, rendering stromal cells more sensitive to apoptosis.<sup>24,27</sup>

In contrast to our results, Schroder et al observed no significant differences in tumor growth in *SerpinB2*<sup>-/-</sup> vs control mice injected with LLC or B16 melanoma cells.<sup>28</sup> Although these data are in direct contrast to those reported here, important differences in the experimental conditions are worth noting. Exclusively 5- to 8-week-old male mice were used in our experiments, whereas Schroder et al performed their experiments exclusively in female mice. Sex significantly affects tumor growth in hepatocellular carcinoma and hepatocarcinogenesis in humans and mice.<sup>29</sup> *SerpinB2* expression in response to lipoprotein(a) has been shown to be sex specific and is only observed in males.<sup>30</sup> Thus, sex could contribute to the disparities in tumor growth rates between these two studies. Additional differences in study design include the site of inoculation (left hind footpad vs subcutaneous back), the numbers of cells used in the inoculation ( $1 \times 10^5$  LLC and B16 melanoma in our study vs  $4\text{--}5 \times 10^5$  used by Schroder et al). In addition, changes in the gut microbiome could play an important role in the differences in tumor growth in experiments performed at different institutions. Mice lacking endothelial specific *Krit1* or *Ccm2* exhibit markedly different manifestations of cerebral cavernous malformation as a function of the gut microbiome, initially uncovered by examination of the same mouse colony in two different vivariums.<sup>31</sup> Because PAI-2 is a stress protein that is highly inducible in activated macrophages and monocytes, similar shifts in microbiome in different laboratories could also potentially influence the host response to an implanted tumor.

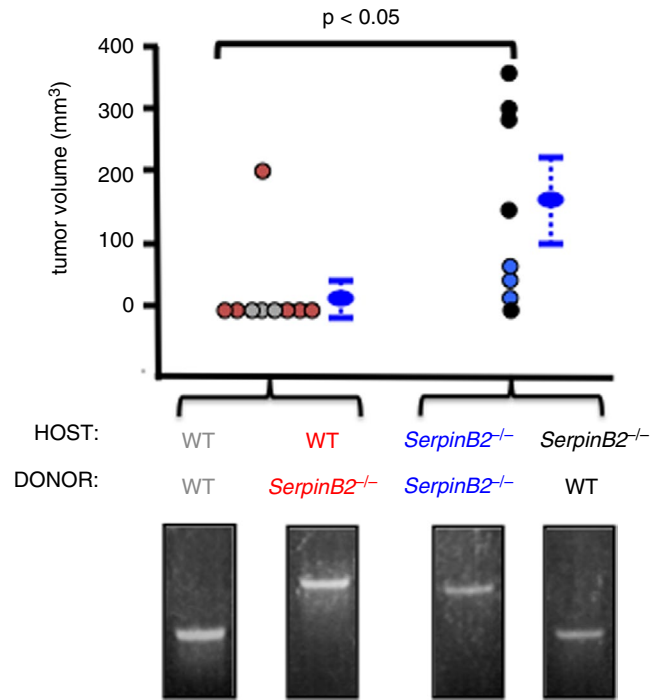


**FIGURE 4** Hematopoietic *SerpinB2*<sup>-/-</sup> does not influence B16 melanoma growth. (MT) experiments were performed using FLCs as a source of hematopoietic stem cells. All surviving mice received footpad B16 melanoma injections 6 weeks post-BMT, and were sacrificed at day 34. Mice with gray symbols represent WT mice receiving WT bone marrow; mice with red symbols represent WT mice receiving *SerpinB2*<sup>-/-</sup> bone marrow. Mice with blue symbols represent *SerpinB2*<sup>-/-</sup> mice receiving *SerpinB2*<sup>-/-</sup> bone marrow. Mice with black symbols represent *SerpinB2*<sup>-/-</sup> mice receiving WT bone marrow. Host *SerpinB2*<sup>-/-</sup> mice receiving WT or *SerpinB2*<sup>-/-</sup> marrow formed significantly larger tumors than the other groups ( $P < .05$ ). Representative samples of *SerpinB2* genotype (by PCR of peripheral blood) following BMT are illustrated, demonstrating engraftment. The upper band represents the *SerpinB2*<sup>-/-</sup> allele and the lower band represents the WT *SerpinB2*<sup>+</sup> allele. Mean footpad tumor volume of *SerpinB2*<sup>-/-</sup> bone marrow recipients was  $160.1 \text{ mm}^3$  vs WT bone marrow recipients,  $24.4 \text{ mm}^3$ ;  $P < .05$ . Bars indicate standard error of the mean for the aggregate tumor volume values based on the host genotype

Taken together, our results suggest that nonhematopoietically derived PAI-2 plays a previously underappreciated role in the response to malignancy. Our findings provide the basis for future studies on the regulation of tumor growth by PAI-2. Investigating the tumor response in mice with specific PAI-2 deficiency in fibroblasts or other stromal cellular constituents<sup>22-26,32</sup> could provide additional insights into the tumorostatic function of PAI-2.

## 4 | Methods

### 4.1 | Mice

WT C57BL/6J (stock #000664) mice were purchased from the Jackson Laboratories. *SerpinB2*-deficient mice generated by gene

targeting as previously reported,<sup>11</sup> were backcrossed for three or seven generations to C57BL/6J (N3, N7) and then intercrossed to generate homozygous null and WT littermate controls. All mice were housed in University of Michigan animal housing facilities, and all experiments were performed in accordance with the University of Michigan animal use guidelines. *Serpinb2* genotype was determined by PCR, as previously described.<sup>11</sup> Male mice between 5 and 8 weeks of age were used in the tumor experiments; the recipient mice used in the transplant experiments were 8-week-old males.

## 4.2 | Tumor cell lines

Both the B16-F1 melanoma (B16 melanoma) and LLC cell lines, originally isolated from a C57BL/6 mouse strain, were purchased from the American Type Culture Collection (#CRL-6323 and #CRL-1642, respectively). All cell lines were maintained in Dulbecco's modified eagle media (Life Technologies) supplemented with 10% fetal calf serum, streptomycin, penicillin, and L-glutamine and were passaged no more than five times.

## 4.3 | Tumorigenic assays

For the tumor inoculations,  $1 \times 10^5$  B16 melanoma or LLC cells in 40  $\mu$ L of sterile Hanks Balanced Salt Solution (HBSS; Invitrogen/ThermoFisher Scientific) were injected into the left hind footpad of each animal in an age-matched cohort of WT and *SerpinB2*-deficient mice after anesthesia with intraperitoneal pentobarbital. All experiments were performed with the operator blinded to the genotype of the mice. For the dorsal intradermal tumor inoculations,  $1 \times 10^5$  LLC cells in 0.1 mL of HBSS were injected. Footpad tumors were monitored for 34 days, at which time tumor size was measured using calipers, and the volumes were calculated using the formula  $(W^2 \times L)/2$  where  $W$  = tumor width and  $L$  = tumor length.<sup>33</sup> This formula approximates the area of an ellipse. After tumor measurement, all animals underwent a left hip disarticulation under anesthesia. Incisions were closed using surgical staples. All animals were subsequently sacrificed 34 days postoperatively to assess lung metastases by gross visual inspection. The thoracic cavity was opened via the removal of the sternum and anterior ribs. The lungs were then inflated via intratracheal injection Fekete's solution and the trachea clamped to prevent backflow. The exterior of the lungs and associated thoracic cavity were visually examined to detect the presence of major lung metastases growing into the chest wall. The respiratory system consisting of the trachea attached to the right and left lungs was then removed from the mice. Surface pulmonary nodules were counted manually, with the examiner blinded to the genotype of the mouse, as previously described.<sup>34</sup>

Mice receiving dorsal intradermal injections of LLC cells were sacrificed 22 days following initial tumor inoculation for tumor

excision and measurement with calipers. Tumor volumes were calculated as described previously.

## 4.4 | Bone marrow transplantation

Fetal livers of both sexes were harvested from WT C57BL/6J and *SerpinB2*<sup>-/-</sup> mice (from an intercross of *SerpinB2*<sup>+</sup> mice N7 on C57BL/6J) as previously described.<sup>35</sup> Briefly, fetal livers were harvested at 18.5 days gestation, homogenized, resuspended in cryo-media (65% Roswell Park Memorial Institute 1640 [RPMI; Invitrogen/ThermoFisher Scientific], 10% dimethylsulfoxide, 25% fetal bovine serum [Invitrogen/ThermoFisher Scientific]), and stored at  $-80^\circ\text{C}$  for future use. Male mice were used as bone marrow recipients. On the day of transplantation, all mice received 1300 cGy of radiation in two divided doses, 3 hours apart. Each mouse received a total of  $5 \times 10^8$  FLCs in a volume of 0.3 mL sterile RPMI via tail vein injection. Four mice received radiation only ("sham-transplanted") followed by tail vein injection of 0.3 mL of sterile RPMI. All mice were then monitored daily and were euthanized at the onset of severe illness (lethargy, ruffled fur). The four sham-transplanted mice died by day 10 after transplant. At 6 weeks posttransplant, surviving mice were injected in the left hind footpad with  $1 \times 10^5$  melanoma cells in 40  $\mu$ L of sterile HBSS, as described previously. On day 34 after tumor injection, all animals were sacrificed to evaluate both primary tumor volume and gross metastatic tumor spread. To assess engraftment of the transplanted mice, DNA was isolated from peripheral blood using the Bio-Rad InstaGene Dry Blood kit, and PCR was performed as previously described.<sup>21</sup>

## 4.5 | Histochemistry

After caliper measurement, tumor specimens were preserved in zinc formalin, and 8- $\mu$ m paraffin sections were stained with hematoxylin and eosin.

## 4.6 | Statistical analysis

The statistical significance of differences between groups was determined by Student's *t* test. Two-sided *P* values of  $<.05$  were considered statistically significant. For the bone marrow transplant experiment, a chi-squared test was used.

## ACKNOWLEDGMENTS

This research was supported by National Institutes of Health grants R35 HL135793 (to D.G.) and R01-HL135035 (to R.J.W.). The Oakland University Research Excellence Fund and American Heart Association Innovative Research grants supported R.J.W. D.G. is a member of the University of Michigan Cancer Center. Research reported in this publication was supported by the National Cancer Institute of the National Institutes of Health under Award Number P30CA046592 by the use

of the following Cancer Center Shared Resource(s): Transgenic Animal Models. We gratefully acknowledge expertise of the Transgenic Animal Model Core staff of the University of Michigan's Biomedical Research Core Facilities for assistance with this study. D.G. is an Investigator of the Howard Hughes Medical Institute.

### CONFLICT OF INTEREST

Each of the authors reports no conflicts of interest for this manuscript.

### AUTHOR CONTRIBUTION

Randal J. Westrick, Lisa Payne Røjkjær, and David Ginsburg designed the research study; Randal J. Westrick, Lisa Payne Røjkjær, and Angela Y. Yang performed the experiments; Randal J. Westrick, Lisa Payne Røjkjær, Angela Y. Yang, Michael H. Roh, Amy E. Siebert, and David Ginsburg analyzed the data; and Randal J. Westrick, Lisa Payne Røjkjær, and David Ginsburg wrote the manuscript, with critical comments from Angela Y. Yang, Michael H. Roh, and Amy E. Siebert.

### ORCID

Randal J. Westrick  <https://orcid.org/0000-0001-8775-8460>

Amy E. Siebert  <https://orcid.org/0000-0002-9634-9164>

### TWITTER

Randal J. Westrick  @WestrickRandal

### REFERENCES

- Mekawaty AH, Morris DL, Pourgholami MH. Urokinase plasminogen activator system as a potential target for cancer therapy. *Future Oncol.* 2009;5(9):1487-1499.
- Croucher DR, Saunders DN, Lobov S, Ranson M. Revisiting the biological roles of PAI2 (SERPINB2) in cancer. *Nat Rev Cancer.* 2008;8(7):535-545.
- Kruihof EK, Tran-Thang C, Gudinchet A, et al. Fibrinolysis in pregnancy: a study of plasminogen activator inhibitors. *Blood.* 1987;69(2):460-466.
- Medcalf RL, Stasinopoulos SJ. The undecided serpin. The ins and outs of plasminogen activator inhibitor type 2. *FEBS J.* 2005;272(19):4858-4867.
- Yoshino H, Endo Y, Watanabe Y, Sasaki T. Significance of plasminogen activator inhibitor 2 as a prognostic marker in primary lung cancer: association of decreased plasminogen activator inhibitor 2 with lymph node metastasis. *Br J Cancer.* 1998;78(6):833-839.
- Ramnefjell M, Aamelfot C, Helgeland L, Akslen LA. Low expression of SerpinB2 is associated with reduced survival in lung adenocarcinomas. *Oncotarget.* 2017;8(53):90706-90718.
- Hanahan D, Coussens LM. Accessories to the crime: functions of cells recruited to the tumor microenvironment. *Cancer Cell.* 2012;21(3):309-322.
- Baker MS, Bleakley P, Woodrow GC, Doe WF. Inhibition of cancer cell urokinase plasminogen activator by its specific inhibitor PAI-2 and subsequent effects on extracellular matrix degradation. *Cancer Res.* 1990;50(15):4676-4684.
- Bugge TH, Kombrinck KW, Xiao Q, et al. Growth and dissemination of Lewis lung carcinoma in plasminogen-deficient mice. *Blood.* 1997;90(11):4522-4531.
- Margalit O, Eisenbach L, Amariglio N, et al. Overexpression of a set of genes, including WISP-1, common to pulmonary metastases of both mouse D122 Lewis lung carcinoma and B16-F10.9 melanoma cell lines. *Br J Cancer.* 2003;89(2):314-319.
- Dougherty KM, Pearson JM, Yang AY, Westrick RJ, Baker MS, Ginsburg D. The plasminogen activator inhibitor-2 gene is not required for normal murine development or survival. *Proc Natl Acad Sci USA.* 1999;96(2):686-691.
- Rudolph KL, Chang S, Lee HW, et al. Longevity, stress response, and cancer in aging telomerase-deficient mice. *Cell.* 1999;96(5):701-712.
- Brayton CF, Treuting PM, Ward JM. Pathobiology of aging mice and GEM: background strains and experimental design. *Vet Pathol.* 2012;49(1):85-105.
- Wang J, Tran J, Wang H, et al. Melanoma tumor growth is accelerated in a mouse model of sickle cell disease. *Exp Hematol Oncol.* 2015;4:19.
- Costelloe EO, Stacey KJ, Antalis TM, Hume DA. Regulation of the plasminogen activator inhibitor-2 (PAI-2) gene in murine macrophages. Demonstration of a novel pattern of responsiveness to bacterial endotoxin. *J Leukoc Biol.* 1999;66(1):172-182.
- Ritchie H, Jamieson A, Booth NA. Regulation, location and activity of plasminogen activator inhibitor 2 (PAI-2) in peripheral blood monocytes, macrophages and foam cells. *Thromb Haemost.* 1997;77(6):1168-1173.
- Shea-Donohue T, Zhao A, Antalis TM. SerpinB2 mediated regulation of macrophage function during enteric infection. *Gut Microbes.* 2014;5(2):254-258.
- Bailey MH, Tokheim C, Porta-Pardo E, et al. Comprehensive characterization of cancer driver genes and mutations. *Cell.* 2018;173(2):371-385 e318.
- Karczewski KJ, Francioli LC, Tiao G, et al. The mutational constraint spectrum quantified from variation in 141,456 humans. *Nature.* 2020; 581(7809):434-443. <https://doi.org/10.1038/s41586-020-2308-7>
- Roszer T. Understanding the biology of self-renewing macrophages. *Cells.* 2018;7(8):103.
- Harris NLE, Vennin C, Conway JRW, et al. SerpinB2 regulates stromal remodelling and local invasion in pancreatic cancer. *Oncogene.* 2017;36(30):4288-4298.
- Mikus P, Ny T. Intracellular polymerization of the serpin plasminogen activator inhibitor type 2. *J Biol Chem.* 1996;271(17):10048-10053.
- Dickinson JL, Bates EJ, Ferrante A, Antalis TM. Plasminogen activator inhibitor type 2 inhibits tumor necrosis factor alpha-induced apoptosis. Evidence for an alternate biological function. *J Biol Chem.* 1995;270(46):27894-27904.
- Tonnetti L, Netzel-Arnett S, Darnell GA, et al. SerpinB2 protection of retinoblastoma protein from calpain enhances tumor cell survival. *Cancer Res.* 2008;68(14):5648-5657.
- Park JM, Greten FR, Wong A, et al. Signaling pathways and genes that inhibit pathogen-induced macrophage apoptosis—CREB and NF-kappaB as key regulators. *Immunity.* 2005;23(3):319-329.
- Delhase M, Kim SY, Lee H, et al. TANK-binding kinase 1 (TBK1) controls cell survival through PAI-2/serpinB2 and transglutaminase 2. *Proc Natl Acad Sci USA.* 2012;109(4):E177-E186.
- Darnell GA, Antalis TM, Johnstone RW, et al. Inhibition of retinoblastoma protein degradation by interaction with the serpin plasminogen activator inhibitor 2 via a novel consensus motif. *Mol Cell Biol.* 2003;23(18):6520-6532.
- Schroder WA, Major LD, Le TT, et al. Tumor cell-expressed SerpinB2 is present on microparticles and inhibits metastasis. *Cancer Med.* 2014;3(3):500-513.
- Naugler WE, Sakurai T, Kim S, et al. Gender disparity in liver cancer due to sex differences in MyD88-dependent IL-6 production. *Science.* 2007;317(5834):121-124.
- Buechler C, Ullrich H, Ritter M, et al. Lipoprotein (a) up-regulates the expression of the plasminogen activator inhibitor 2 in human blood monocytes. *Blood.* 2001;97(4):981-986.

31. Tang AT, Choi JP, Kotzin JJ, et al. Endothelial TLR4 and the microbiome drive cerebral cavernous malformations. *Nature*. 2017;545(7654):305-310.
32. Bodenstine TM, Seftor RE, Khalkhali-Ellis Z, Seftor EA, Pemberton PA, Hendrix MJ. Maspin: molecular mechanisms and therapeutic implications. *Cancer Metastasis Rev*. 2012;31(3-4):529-551.
33. O'Reilly MS, Pirie-Shepherd S, Lane WS, Folkman J. Antiangiogenic activity of the cleaved conformation of the serpin antithrombin. *Science*. 1999;285(5435):1926-1928.
34. Eitzman DT, Krauss JC, Shen T, Cui J, Ginsburg D. Lack of plasminogen activator inhibitor-1 effect in a transgenic mouse model of metastatic melanoma. *Blood*. 1996;87(11):4718-4722.
35. Fazio S, Babaev VR, Murray AB, et al. Increased atherosclerosis in mice reconstituted with apolipoprotein E null macrophages. *Proc Natl Acad Sci USA*. 1997;94(9):4647-4652.

**How to cite this article:** Westrick RJ, Røjkjær LP, Yang AY, Roh MH, Siebert AE, Ginsburg D. Deficiency of plasminogen activator inhibitor-2 results in accelerated tumor growth. *J Thromb Haemost*. 2020;18:2968–2975. <https://doi.org/10.1111/jth.15054>